

Article

Hydrothermal Oxidation of Coarse Aluminum Granules with Hydrogen and Aluminum Hydroxide Production: The Influence of Aluminum Purity

Grayr N. Ambaryan ^{1,*}, Olesya A. Buryakovskaya ¹, Vinod Kumar ^{2,3}, Georgii E. Valyano ¹,
Elena A. Kiseleva ¹, Anatoly V. Grigorenko ¹ and Mikhail S. Vlaskin ^{1,*}

¹ Joint Institute for High Temperatures, Russian Academy of Sciences, 125412 Moscow, Russia; osminojishe@yandex.ru (O.A.B.); gvalyano@yandex.ru (G.E.V.); kanna787@mail.ru (E.A.K.); presley1@mail.ru (A.V.G.)

² Algal Research and Bioenergy Lab, Department of Food Science and Technology, Graphic Era (Deemed to be University), Dehradun 248002, India; vinodkdhatwalia@gmail.com

³ Department of Environmental Safety and Product Quality Management, Peoples' Friendship University of Russia Named after Patrice Lumumba, 117198 Moscow, Russia

* Correspondence: ambaryan1991@gmail.com (G.N.A.); vlaskin@inbox.ru (M.S.V.)

Abstract: This study is devoted to the hydrothermal oxidation of aluminum—the exothermic process in which hydrogen and aluminum oxide (or hydroxide) are produced. In this work, the influence of the chemical purity of aluminum on the conversion degree of coarse aluminum at hydrothermal oxidation was studied. Distilled water and coarse granules of aluminum with an average size of ~7–10 mm and three different aluminum purities—99.7, 99.9, and 99.99%—were used in the experiments. The oxidation experiments were carried out inside a 5 liter autoclave in an isothermal mode at temperatures from 200 to 280 °C, with a step of 20 °C. The holding time at the set temperature varied from 4 to 10 h. It was shown that the chemical purity of aluminum considerably influences the oxidation kinetics. More chemically pure aluminum oxidizes much faster, e.g., at a temperature of 280 °C and a holding time of 10 h, the conversion degree of granules with a chemical purity of 99.9% and 99.7% was less than 2%, while 99.99% aluminum was almost fully oxidized. The conversion degree of 99.99% aluminum decreased with the reduction in temperature and holding time, to 66–68% at 280 °C, 4 h, and 2–3% at 200 °C, 10 h.

Keywords: hydrogen; hydrogen generation; hydrogen-containing materials; chemical impurities; boehmite; hydrothermal oxidation; oxidation of aluminum; conversion efficiency



Citation: Ambaryan, G.N.; Buryakovskaya, O.A.; Kumar, V.; Valyano, G.E.; Kiseleva, E.A.; Grigorenko, A.V.; Vlaskin, M.S. Hydrothermal Oxidation of Coarse Aluminum Granules with Hydrogen and Aluminum Hydroxide Production: The Influence of Aluminum Purity. *Appl. Sci.* **2023**, *13*, 7793. <https://doi.org/10.3390/app13137793>

Academic Editors: Rafael F.A. Gomes and Svilen P. Simeonov

Received: 29 May 2023

Revised: 20 June 2023

Accepted: 27 June 2023

Published: 1 July 2023



Copyright: © 2023 by the authors. Licensee MDPI, Basel, Switzerland. This article is an open access article distributed under the terms and conditions of the Creative Commons Attribution (CC BY) license (<https://creativecommons.org/licenses/by/4.0/>).

1. Introduction

Hydrogen is increasingly recognized as a potential fuel of the future, primarily due to its eco-friendly combustion that does not result in carbon emissions. Despite being a secondary fuel that must be produced and stored using hydrogen storage materials [1,2], it exhibits significant potential for sustainable energy solutions. The prevalent industrial method for hydrogen production, the steam reforming of natural gas, generates significant carbon dioxide emissions [3], contradicting the goals of low-carbon energy strategies.

Electrolysis, when powered by low-carbon energy sources, such as renewable sources, hydroelectric plants, or nuclear plants, offers a low-carbon hydrogen production solution. However, despite advancements in electrolysis technologies, their unit capacity remains somewhat limited.

In light of this, research has explored aluminum hydrolysis for hydrogen production. This holds particular applications in low power proton exchange membrane fuel cells, where mechanochemically activated Al composites using bismuth (Bi) and nickel (Ni) as activating compounds have been utilized [4].

An alternative approach to generating sustainable hydrogen involves the oxidation of aluminum in water. This process benefits from the established technologies of the aluminum industry and, unlike electrolysis, does not require distilled water. Oxidizing a kilogram of aluminum in water yields approximately 15.5 MJ of thermal energy and 111 g of hydrogen, with an additional energy potential of 15.5 MJ. A challenge in this process is the formation of an oxide film on the aluminum surface during oxidation, which impedes efficiency [5]. Most of the previous research has been devoted to the search for chemical additives to solve this issue in order to enhance the oxidation rate and the aluminum conversion degree.

Previous studies have investigated the use of chemical additives for addressing this issue, including the use of alkalis [6–10] or salts [11] in aqueous solutions, as well as the activation of aluminum by various metals, silicon, graphite, chlorides, and oxides [12–26]. Xinren Chen et al. have demonstrated a unique aluminum corrosion mechanism, which could have promising implications for its use in energy production [27].

Another relevant aspect in the production of hydrogen through aluminum oxidation is the utilization of dopants and alloying additives. Recent research by Buryakovskaya et al. [28] highlighted the possibility of using a combination of oxidation mediums, ball milling parameters, and copper additives to ensure a fast reaction of aluminum scrap with a high hydrogen yield.

In the study by Buryakovskaya et al., aluminum was alloyed with copper to form an Al-10 wt.% Cu composition. Different milling parameters were tested, including the size of the steel balls (5, 10, and 15 mm), the milling time (1 and 2 h), and the rotation modes. The samples milled with 5 mm (2 h) and 10 mm balls (1 and 2 h) were found to contain undesired intermetallic phases Al_2Cu and Cu_9Al_4 , while the samples activated with 15 mm balls (1 h) showed the best preservation of the original Cu and Al phases.

Furthermore, the study tested various oxidation mediums at 60 °C, including 2M solutions of NaCl, LiCl, KCl, MgCl_2 , ZnCl_2 , BaCl_2 , CaCl_2 , NiCl_2 , CoCl_2 , FeCl_2 , and AlCl_3 . Of these, AlCl_3 yielded the highest hydrogen production, reaching 91.5%.

Different samples with varying Cu dispersity were milled under optimal parameters and tested in AlCl_3 . The total hydrogen yields were similar across the samples (~90–94%); however, the reaction rates varied, with the highest rate obtained for the sample modified with 50–70 μm powder.

In contrast to the chemical additive approach, some researchers have proposed a hydrothermal oxidation method for oxidizing non-activated aluminum in pure water [29–32]. This method utilized a vertical continuous flow reactor in distilled water at temperatures of 300–350 °C and pressures of 10–15 MPa. The method was sensitive to the particle size of the aluminum powder [33], with larger particles used in the experimental plant up to 40 μm [34]. A key drawback was that tiny aluminum particles could clog valves and pipes, posing technical and safety challenges under high-pressure and high-temperature conditions.

Coarse aluminum could offer a cost-effective alternative to aluminum powders, given that fine aluminum powders can be considerably more expensive than aluminum ingots, depending on the powder dispersion. A recent study demonstrated the feasibility of completely oxidizing aluminum granules of about 1 cm in size [35]. However, this study suggested that the oxidation process might be affected by the state of the water (liquid or steam). In the present study, we aim to examine this assumption by conducting a series of oxidation experiments on aluminum granules in a 5 L autoclave reactor. We also examine the influence of aluminum's chemical purity on the hydrothermal oxidation process, a topic not previously explored. Additionally, this investigation examines the impact of aluminum's chemical purity on the process of hydrothermal oxidation, a topic that has not previously been extensively explored. This research focus is based on previous findings indicating that the chemical composition of both aluminum and water significantly influences the oxidation process.

While this research delves into the study of aluminum oxidation in both liquid water and steam within the same experimental setup, it also investigates a more cost-effective

approach using coarse aluminum. The study offers a comprehensive examination of aluminum hydrothermal oxidation, exploring parameters such as aluminum granule size and oxidation rates in different states of water.

Furthermore, this research seeks to address challenges related to the use of fine aluminum powder in oxidation processes. The tendency of fine aluminum particles to clog valves and pipes presents significant safety and operational concerns in high-pressure and high-temperature environments.

By comparing the conversion degrees from these experiments, this study strives to obtain deeper insights into the role of aluminum purity and water state in aluminum hydrothermal oxidation. The ultimate goal is to enhance our understanding of efficient hydrogen production using sustainable methods, contributing to the larger scientific discourse on low-carbon energy strategies.

Our findings have the potential to drive advancements in the hydrogen production sector, facilitating more eco-friendly and efficient processes that align with the goals of sustainable energy development.

2. Materials and Methods

2.1. Initial Reagents

In the experiments, aluminum in the form of granules of three different chemical purities was used. The aluminum granules selected possessed an aluminum content of 99.7% (grade A7), 99.9% (grade A9), and 99.99% (grade A99). All aluminum granules were received from UC Rusal. The photo of the aluminum granules is shown in Figure 1. The size of the aluminum granules used in the experiments was ~7–10 mm. Distilled water was used to carry out the oxidation process of the aluminum granules.

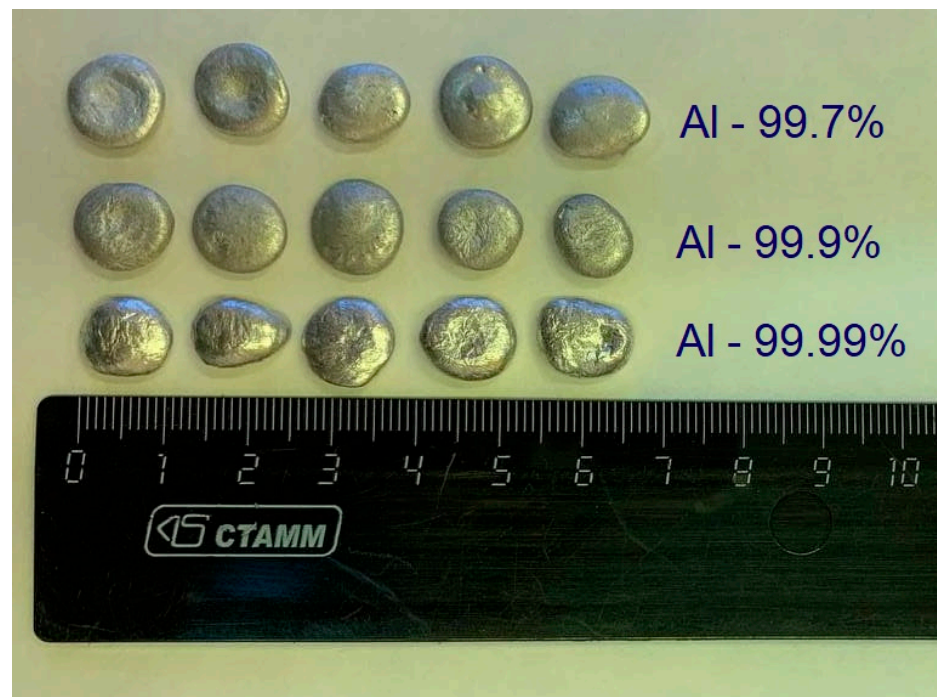


Figure 1. Photo of aluminum granules used in hydrothermal oxidation experiments.

2.2. Experimental Plant

The study of the oxidation processes of aluminum in the form of granules with different chemical purities in heated liquid water and steam was carried out on an experimental installation, which is shown in Figure 2a.

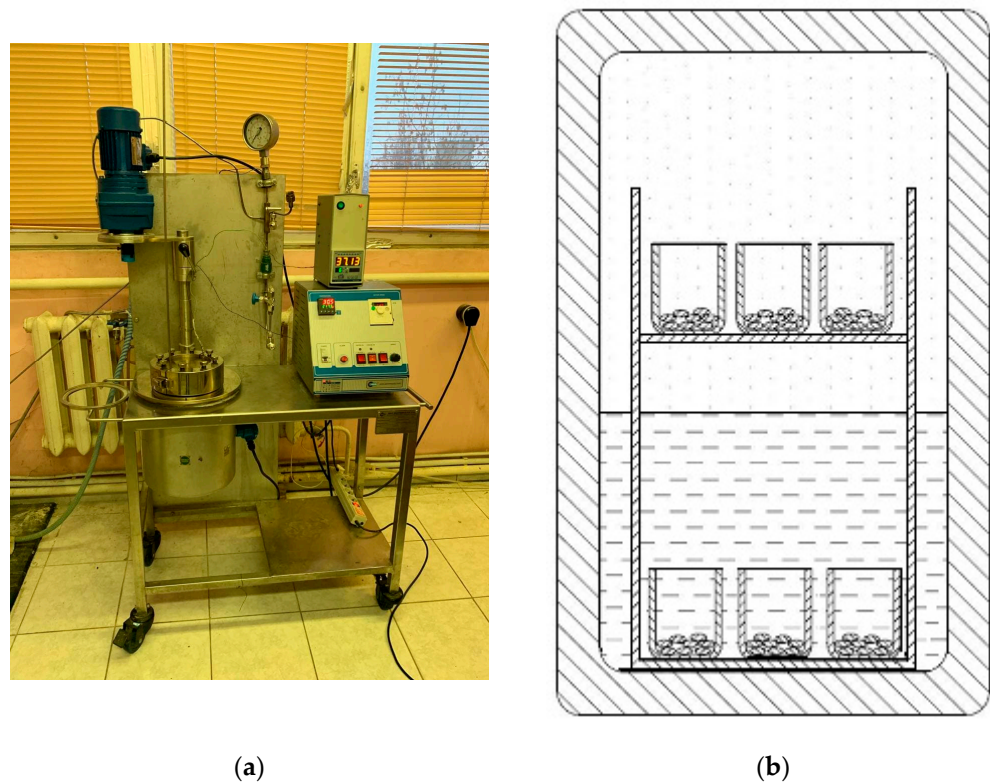


Figure 2. (a) Photo of a laboratory installation for the study of the oxidation process of aluminum granules; (b) layout of crucibles with aluminum granules with water inside a heated autoclave reactor during the oxidation experiment (liquid water from the bottom of the reactor, steam from the top of the reactor). On top (in steam) and on the bottom (in liquid water), there are three crucibles with three samples of aluminum with different chemical purities (99.7, 99.9, and 99.99%).

The autoclave, with an internal volume of 5 L, is made of SS 316 stainless steel with a ceramic belt heater. The reactor is thermally insulated. The temperature is regulated by a controller, which ensures a constant temperature inside the reactor. Inside the autoclave reactor, there is a two-level stand, the scheme of which is shown in Figure 2b, on which ceramic crucibles with aluminum granules of a given mass are placed. The stand is designed to accommodate crucibles at different levels inside the reactor, making it possible to simultaneously carry out the oxidation process in water (from the bottom of the reactor) and steam (from the top of the reactor). On top (in steam) and on the bottom (in liquid water), there are three crucibles with three samples of aluminum with different chemical purities.

During the experiment, the temperature and pressure inside the reactor is recorded with the help of a resistance thermometer and a pressure sensor, respectively. The readings of both devices are recorded using a multichannel thermometer TM 5103 ('Elemer' LLC, Podolsk, Russia), then transferred to a computer for visualization and analysis of the data received.

2.3. Oxidation Experiments

In each experiment, ~2 L of distilled water were poured into the reactor. Before the oxidation experiment, the aluminum granules were initially processed in an ultrasonic bath. Ultrasonic treatment was used to clean the surface of the granules of organic and mechanical impurities. After that ~3–3.5 g of aluminum granules were poured into each ceramic crucible, the crucibles were installed on a two-level stand. Inside the reactor, there were three ceramic crucibles on the lower tier (in steam) and three crucibles on the upper tier (in liquid water). There were three different grades of aluminum granules on each tier of a two-level stand. After installing a two-level stand in the reactor, a thin layer of heat-resistant sealant (Done Deal) was applied to the groove of the reactor lid and the joints

with the surface of the cylindrical tank of the autoclave reactor. The sealing of the system was carried out after installing the flange mount on the autoclave lid, and the uniform tightening force of all bolts was controlled using a torque wrench. After the installation of all measuring devices, the reactor heating system was activated, and the achievement of the set temperature and heating time was recorded. The experimental study of the oxidation of aluminum granules was maintained in an isothermal mode with exposure at a set temperature ranging from 200 to 280 °C, with an increasing step of 20 °C. The holding time at the set temperature begins from 4 to 10 h, in 2 h increments. In the experiments, the average heating time to achieve the set temperature was ~1.5 h. After reaching the set reaction time, the temperature maintenance in the reactor was discontinued, and there was a gradual cooling. The product obtained after the oxidation process was sent to a BINDER drying oven ('BINDER' GmbH, model ED 56, Tuttlingen, Germany) for heat treatment, in which the sample was dried at a temperature of 120 °C, and the mass of the solid oxidation product formed in each crucible was measured.

2.4. X-ray Analysis

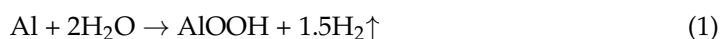
The phase composition of the samples was studied by X-ray diffraction on a SmartLabSE—Rigaku (Tokyo, Japan) diffractometer using CuK α radiation according to the Rietveld method. X-ray diffraction spectra were recorded in the range of angles $2\theta = 10\text{--}90^\circ$, with a scanning step of 0.02 degrees. The phase composition of the samples was identified using the SmartLab Studio II software (version 4.3). The coherent scattering region was calculated using the Scherrer equation.

2.5. Scanning Electron Microscopy (SEM)

The surface morphology of the samples was studied on a NOVA NanoSem 650 (FEI Co., Hillsboro, OR, USA) scanning electron microscope (SEM) using a ring backscattered electron detector, which makes it possible to obtain contrast on the relief surfaces using the average atomic numbers of the microstructure elements. The samples were attached to the microscope stage using an electrically conductive tape. The samples were not coated with a conductive coating to avoid the possible shielding of nanoscale objects. The scanning was carried out by secondary electrons with accelerating voltages of 2 and 3 kV. To reduce the inevitable charging of the samples by the electron probe, SEM images were obtained by multiple scans using the “drift correction” mode.

3. Results and Discussion

A series of experiments conducted in an autoclave with aluminum granules of various purities were performed to study and evaluate the dependence of the degree of aluminum transformation on various experimental conditions, such as temperature, holding time, the state of water (liquid or steam), and the initial chemical purity of the aluminum granules. After the experiment, the oxidized product is a white crystalline compound. The chemical reaction is described by the formula:



In the process of oxidation, the destruction of granules of various degrees occurs. The destruction can be grouped according to the nature of the changes: (a) complete or nearly complete transformation of metallic aluminum into boehmite powder, with minor inclusions (residues) of metallic aluminum; (b) firmly glued pieces of aluminum and boehmite; or (c) granules on which the oxidation process occurred only on the surface, without visible changes or deformation of the granule itself.

The resulting boehmite after oxidation is practically impossible to separate from the metallic inclusions of aluminum, which were not oxidized during the experiment. The

method for calculating the conversion degree was based on the mass measurements. It was carried out, taking into account two different compounds, boehmite and metallic aluminum:

$$\begin{cases} x + y = z \\ x + 2.22y = c \end{cases} \quad (2)$$

where, x —is the mass of non-oxidized aluminum after the oxidation experiment (in the form of metallic inclusions), y —is the mass of oxidized aluminum after the oxidation experiment, z —is the mass of the initial metallic aluminum, and c —is the final mass of the solid product (non-oxidized aluminum + boehmite).

$$z - y + 2.22y = c \quad (3)$$

the coefficient 2.22 is the mass (in g) of the complete transformation of 1 g of aluminum into boehmite (AlOOH) in accordance with the reaction (1); 2.22 y is the mass of boehmite obtained in the reaction.

$$y = \frac{c - z}{1.22} \quad (4)$$

Parameters c and z were measured during the experiments. The conversion degree of aluminum was determined by the formula:

$$\eta[\%] = \frac{y \times 100}{z} \quad (5)$$

3.1. Effect of Temperature on the Conversion Degree of Aluminum

The first series of experiments was carried out to establish the dependence of the conversion degree of aluminum on the reaction temperature. The set temperature was increased with a step of 20 °C, and the experiments were carried out in the temperature range of 200 °C to 280 °C. The results of these experiments are presented in Table 1. The holding time in all these experiments was 10 h.

Table 1. Conversion degree of aluminum (η) in experiments at temperatures from 200 to 280 °C. The holding time in all experiments was 10 h.

N ^o Exp.	T, °C	State of Water	Chemical Purity of Aluminum, %	z, g	c, g	h, %	V(H ₂), L
1	200	Steam	99.99	3.07	3.14	1.87	0.07
			99.9	3.14	3.15	0.26	0.01
			99.7	3.26	3.27	0.25	0.01
		Liquid	99.99	3.06	3.17	2.95	0.11
			99.9	3.19	3.21	0.51	0.02
			99.7	3.21	3.22	0.26	0.01
2	220	Steam	99.99	3.11	3.33	5.80	0.22
			99.9	3.10	3.11	0.26	0.01
			99.7	3.18	3.18	0.00	0.00
		Liquid	99.99	3.09	3.37	7.43	0.29
			99.9	3.06	3.08	0.54	0.02
			99.7	3.16	3.17	0.26	0.01

Table 1. Cont.

N ^o Exp.	T, °C	State of Water	Chemical Purity of Aluminum, %	z, g	c, g	h, %	V(H ₂), L
3	240	Steam	99.99	3.06	3.97	24.38	0.93
			99.9	3.24	3.26	0.51	0.02
			99.7	3.24	3.24	0.00	0.00
		Liquid	99.99	3.01	4.33	35.95	1.35
			99.9	3.19	3.22	0.77	0.03
			99.7	3.33	3.35	0.49	0.02
4	260	Steam	99.99	3.25	5.97	68.60	2.78
			99.9	3.26	3.28	0.50	0.02
			99.7	3.16	3.16	0.00	0.00
		Liquid	99.99	3.25	6.27	76.17	3.08
			99.9	3.23	3.28	1.27	0.05
			99.7	3.19	3.20	0.26	0.01
5	280	Steam	99.99	3.11	6.78	96.73	3.75
			99.9	3.02	3.05	0.81	0.03
			99.7	3.05	3.06	0.27	0.01
		Liquid	99.99	3.06	6.79	100.0	3.81
			99.9	3.11	3.16	1.32	0.05
			99.7	3.00	3.00	0.00	0.00

z—the mass of the initial metallic aluminum; c—the final mass of the solid product (non-oxidized aluminum + boehmite); V(H₂)—the volume of generated hydrogen in the reaction, liters.

The results show that (Figure 3), with an increase in temperature, the oxidation of aluminum in liquid water proceeds better than that in steam. Granules with a chemical purity of 99.99% were completely oxidized at 280 °C in liquid water. The graph based on the results of the experiment shows that the oxidation up to 220 °C in liquid and in steam is the same, but above 220 °C, the conversion degree (η) curve in a liquid is accelerated in comparison with the steam curve under the same conditions. Aluminum with a chemical purity of 99.9% retains the same tendency relative to the oxidation medium, but essentially does not oxidize compared to aluminum with a chemical purity of 99.99%; the conversion degree of aluminum granules with a chemical purity of 99.7% was less than 0.5%.

3.2. Effect of Holding Time on the Conversion Degree of Aluminum

The next series of experiments was carried out to establish the dependence of the conversion degree of aluminum on the holding time of the oxidation reaction. The experiments were carried out with a holding time of 4, 6, 8, and 10 h. The oxidation experiments were carried out in an isothermal mode, and the set temperature in all experiments was 280 °C.

From the results presented in Table 2, it can be seen that at a set point of 4 h, the degree of conversion of aluminum within liquid is slightly lower (~2.4%) compared to the oxidation in steam. At a holding time 6, 8, and 10 h, the conversion degree of aluminum in liquid is higher as compare to that in steam (for aluminum with a chemical purity of 99.99%). The conversion degree (η) curve in a liquid is smoother compared to the steam curve, which proceeds with local acceleration, as seen in Figure 4.

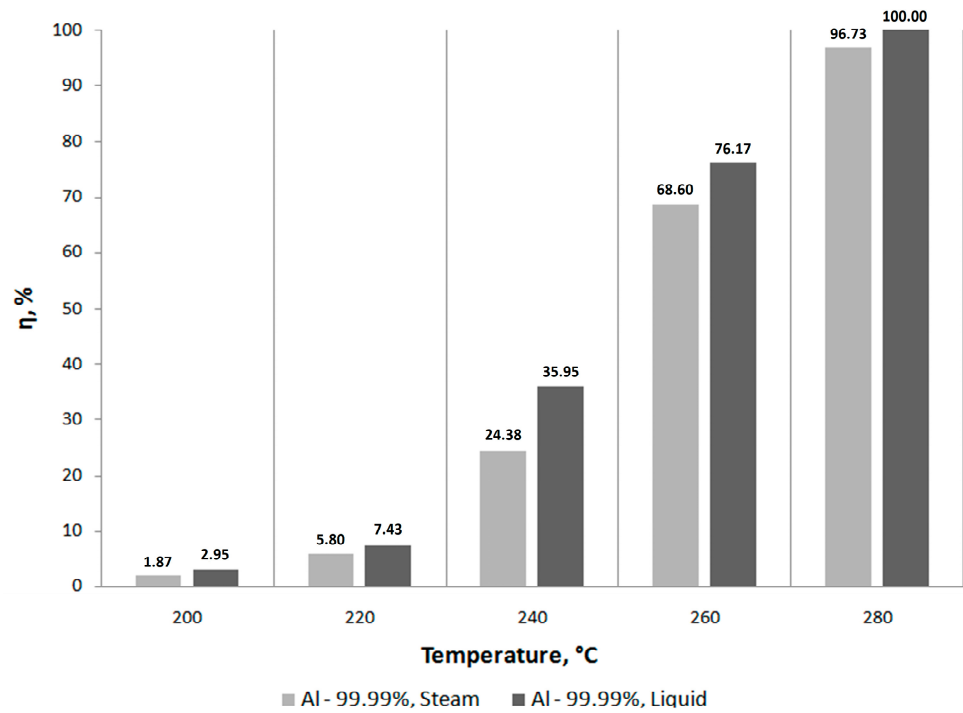


Figure 3. The dependence of the conversion degree of aluminum with a chemical purity of 99.99% on the temperature in steam and liquid; the holding time is 10 h.

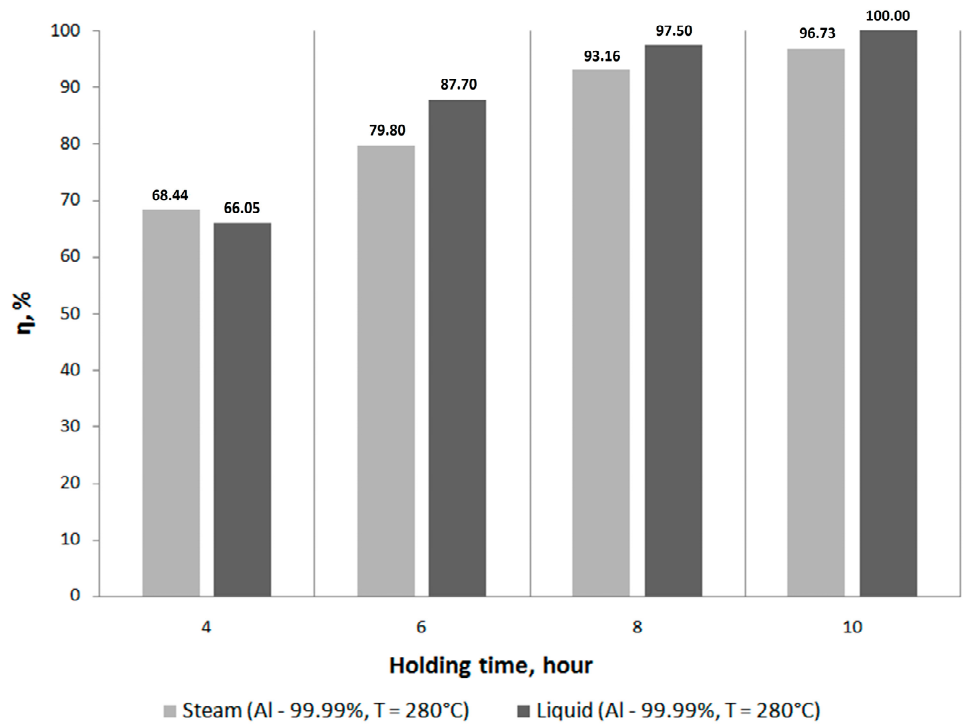


Figure 4. The dependence of the conversion degree of aluminum with a chemical purity of 99.99% on the holding time at a temperature of 280 °C.

Table 2. Conversion degree of aluminum (η) in experiments at a temperature of 280 °C with a holding time from 4 to 10 h.

№ Exp.	Holding Time, Hours	State of Water	Chemical Purity of Aluminum, %	z , g	c , g	h , %	$V(H_2)$, L
1	4	Steam	99.99	2.97	5.45	68.44	2.53
			99.9	3.00	3.04	0.96	0.04
			99.7	3.14	3.15	0.26	0.01
		Liquid	99.99	2.91	5.26	66.05	2.40
			99.9	3.14	3.19	1.31	0.05
			99.7	3.15	3.15	0.00	0.00
2	6	Steam	99.99	3.02	5.96	79.80	3.00
			99.9	3.02	3.08	1.63	0.06
			99.7	2.99	3.00	0.27	0.01
		Liquid	99.99	3.00	6.21	87.70	3.28
			99.9	2.99	3.05	1.64	0.06
			99.7	3.02	3.16	3.80	0.14
3	8	Steam	99.99	3.15	6.73	93.16	3.65
			99.9	3.07	3.09	0.53	0.02
			99.7	3.14	3.14	0.00	0.00
		Liquid	99.99	3.06	6.70	97.50	3.72
			99.9	3.05	3.09	1.07	0.04
			99.7	3.09	3.10	0.27	0.01
4	10	Steam	99.99	3.11	6.78	96.73	3.75
			99.9	3.02	3.05	0.81	0.03
			99.7	3.05	3.06	0.27	0.01
		Liquid	99.99	3.06	6.79	100.0	3.81
			99.9	3.11	3.16	1.32	0.05
			99.7	3.00	3.00	0.00	0.00

z —the mass of the initial metallic aluminum; c —the final mass of the solid product (non-oxidized aluminum + boehmite); $V(H_2)$ —the volume of generated hydrogen in the reaction, liters.

When oxidizing other grades of aluminum, the conversion degree is at the level of error and does not exceed 2%, which does not allow for the interpretation of the results of these experiments.

3.3. Effect on Alloying Additives and Dopants to Increase Hydrogen Production

A study involving Al–Mg–Ga–In–Sn alloys demonstrated another perspective on the utilization of alloying additives [36–38]. These alloys were prepared using arc melting and melt-spinning techniques, and their microstructures were analyzed. The study found that magnesium's effect on the water splitting reaction of aluminum was mainly due to the induction of segregation of indium and tin, as well as the formation of intermetallic compounds on the aluminum surfaces. Moreover, the refinement of aluminum grains in the rapidly solidified alloys significantly enhanced the reaction rate and hydrogen yield. Interestingly, magnesium dissolved in aluminum grains showed negligible effects on the reaction. This finding suggests that the microstructural properties of the alloys can be a critical factor in enhancing hydrogen production through aluminum–water reactions.

Another study focusing on Al–Cu–Ga–In–Sn alloys produced by smelting and casting evaluated the influence of copper on the water–aluminum reaction [39,40]. The findings

indicated that copper impedes the reaction, primarily due to the formation of Al_2Cu . This compound precipitated at the aluminum grain boundaries, affecting the formation and distribution of the low melting point Ga-In-Sn phase. This precipitation also interrupted the direct contact between the aluminum matrix grain and the Ga-In-Sn phase at the interface, resulting in a decrease in reaction rate and hydrogen yield. This highlights the significance of careful alloying element selection and composition, as certain alloying elements, such as copper, may have a detrimental effect on hydrogen production from aluminum–water reactions [41].

Another line of research has investigated the production of hydrogen using aluminum waste can powder (AWCP). AWCP and its composites were subjected to disintegration and mechanochemical activation using metals. When reacted in 1M NaOH under standard temperature conditions, a ternary AWCP (3% Sn–3% Mg) composite produced the highest amount of hydrogen, in terms of weight percentage, compared to a binary AWCP. Activation metals were found to contribute to microgalvanic activity in AWCP, which in turn led to higher hydrolysis rates. Additionally, the hydrogen produced from the aluminum–water reaction was successfully used to produce methane through a continuous methanation process. This research demonstrates the potential of AWCP as a raw material for hydrogen production and opens up possibilities for producing clean, sustainable, and economically viable energy through simultaneous methanation [42].

Based on the results of the research cited above, we suggest that by optimizing the dopants and alloying additives, it is possible to manipulate the reaction rates and enhance hydrogen production. This approach offers an alternative pathway for increasing hydrogen production efficiency, complementing the findings regarding the influence of aluminum purity, temperature, and holding time previously discussed in this article.

3.4. Influence of Changes in the Structure and Morphology of Aluminum on Hydrothermal Oxidation

Structural and morphological changes can significantly affect the efficiency of the hydrothermal oxidation process, and the presence of impurities on the aluminum surface further complicates process.

When aluminum is alloyed with elements such as magnesium (as seen in the Al-Mg-Ga-In-Sn alloys), the formation of intermetallic compounds on the surface of aluminum is observed. These compounds are attributed to the segregation of elements such as indium and tin. Interestingly, these intermetallic compounds seem to play a role in enhancing the rate of hydrothermal oxidation by altering the surface properties of aluminum. However, the mere dissolution of magnesium into aluminum grains was observed to have no significant impact on the reaction. This suggests that the surface-bound compounds and segregations substantially influence the reaction kinetics.

Conversely, in the case of copper alloyed with aluminum (Al-Cu-Ga-In-Sn), the formation of intermetallic compounds such as Al_2Cu at the grain boundaries adversely affects the reaction. The formation of these compounds interrupts the direct contact between the aluminum matrix and the other alloyed phases, thereby inhibiting the reaction. This shows that not all alloying elements and their resultant compounds are beneficial; some can indeed have detrimental effects on the hydrothermal oxidation process.

Furthermore, the presence of impurities, such as oxides or other unwanted compounds on the surface of aluminum, poses challenges in achieving efficient hydrothermal oxidation. These impurities can act as barriers, hindering the contact between aluminum and water. Consequently, the reaction rates can be reduced. For efficient hydrogen production through hydrothermal oxidation, it is critical to either minimize these surface impurities or employ strategies such as mechanochemical activation, as seen in the case of aluminum waste can powder (AWCP), to overcome these barriers.

In summary, changing the structure and morphology of aluminum through alloying and other means can have both positive and negative impacts on hydrothermal oxidation. The presence of impurities or certain intermetallic compounds on the surface can hinder the oxidation process. Understanding and controlling the microstructure of aluminum and its

alloys is crucial for optimizing its hydrothermal oxidation for hydrogen production. This calls for a meticulous selection of alloying elements and processing conditions to favorably tailor the surface properties.

3.5. Influence of the Size and Shape of Aluminum Granules on Hydrothermal Oxidation

The size and shape of the aluminum granules can indeed have a significant impact on the oxidation process. This is because these factors largely determine the surface area of the aluminum that is in contact with water, which directly influences the reaction rate of the oxidation process.

The reaction between aluminum and water is a surface-dependent process. Therefore, the larger the surface area of the aluminum that is exposed to water, the faster the reaction can proceed. Consequently, smaller granules, which have a larger surface-to-volume ratio compared to larger granules, are likely to oxidize more quickly. This is because more of the aluminum atoms are available for reaction with water.

In terms of shape, irregular or non-spherical granules often have a greater surface area compared to spherical granules of the same volume. This could lead to faster oxidation rates in non-spherical granules. However, irregularly shaped granules may also have surface recesses or crevices where water may not readily reach, potentially slowing the oxidation process in these areas.

Both these effects—granule size and shape—can lead to variability in the oxidation process, making it more challenging to predict and control. Therefore, to account for these effects, a correction factor or error value might need to be introduced when modeling or predicting the oxidation process based on granule size and shape.

This correction factor or error value could be determined empirically, and the experimental results could then be compared with the theoretical predictions. By so doing, one could quantify the degree to which size and shape influence the oxidation process and then use this information to adjust the predictions accordingly.

It should be noted that such a correction factor or error value would likely be specific to the conditions under which the oxidation process is being conducted. Factors such as temperature, pressure, and the presence of other substances (e.g., impurities in the aluminum or additives in the water) could also influence the oxidation process and would need to be accounted for when determining the correction factor or error value.

Therefore, while the size and shape of aluminum granules can significantly influence the oxidation process, quantifying this influence is complex and requires careful experimental design and analysis. However, with such information, one could make more accurate predictions about the oxidation process and thus improve the efficiency and control of applications in which the hydrothermal oxidation of aluminum is used.

3.6. Results of X-ray and SEM Analysis

The obtained samples of the solid product were analyzed for phase composition, and the results are shown in Figure 5.

The presence of the main phase, AlOOH (boehmite) with a rhombic lattice structure, in both samples indicates that the hydrothermal oxidation reaction is successfully producing the expected product. Boehmite is a well-known aluminum oxide hydroxide phase and is typically produced when aluminum reacts with water under hydrothermal conditions. However, the presence of another phase, χ -Al₂O₃, in the samples is noteworthy. χ -Al₂O₃ is another phase of aluminum oxide that typically forms at high temperatures.

The distinction in the prominence of χ -Al₂O₃ phase at 48 and 67 degrees (2 Theta) in the sample obtained with steam suggests that the conditions during the steam-based hydrothermal oxidation are conducive to the formation of this phase. This could be due to the higher energy state of water in steam form, which could facilitate the formation of χ -Al₂O₃ through a different pathway, or due to a change in the thermodynamics of the system.

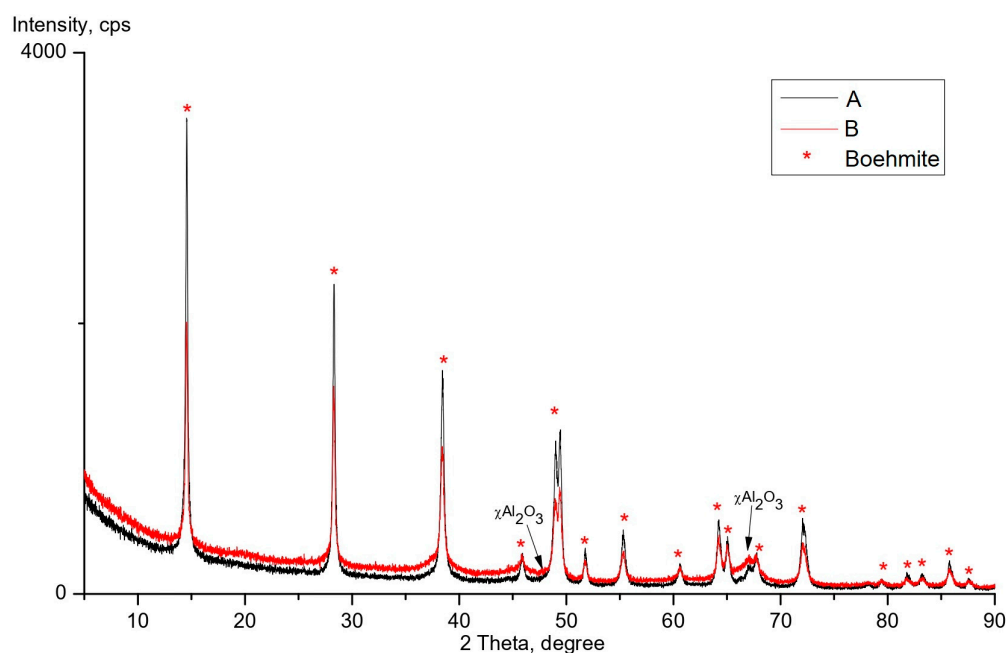


Figure 5. The results of X-ray analysis of boehmite obtained by the oxidation of aluminum with a chemical purity of 99.99% at 280 °C and 10 h: A—in liquid; B—in steam.

Furthermore, the presence of metallic aluminum inclusions in the samples obtained with steam indicates that the oxidation process is not complete. This might be attributed to the fact that steam, being in the gas phase, does not have as intimate contact with the aluminum surface, as does liquid water. Additionally, the higher kinetic energy of steam might lead to less effective mass transfer to the aluminum surface, which can hinder the oxidation process. This, in turn, leads to a product that is a mixture of different phases with a somewhat heterogeneous structure due to varying grain parameters.

The difference in grain parameters between the phases could have significant implications for the mechanical and chemical properties of the resultant material. For example, different grain sizes and structures can affect the material's strength, hardness, porosity, and chemical reactivity. These properties are crucial in applications such as catalysis, structural materials, and energy storage.

A series of SEM images was also obtained to study the microstructure of the oxidation product. Figure 6 shows SEM images of boehmite samples obtained in oxidation experiments with 99.99% aluminum. From the analysis of the images, it follows that an increase in the conversion degree of aluminum (η) leads to the formation of macropores (with a pore diameter of more than 50 nm) on the surface of the sample where the conversion degree (η) is greater than 95% (on a scale of 50 μm , Figure 6). The surface of the particles (e), (f) and (g), (h), where $\eta < 70\%$, is denser, without visible macropores. This is clearly seen in the image of the sample (h) 5 μm , as the observed surface is monolithic without crystalline inclusions; the degree of transformation (η) of this sample is 24.38%.

Figure 7 shows photos of boehmite samples obtained by the oxidation of aluminum with a chemical purity of 99.99%. The sample in Figure 7a is oxidized in a liquid with the conversion degree of 100.0% and exhibits a white color characteristic of boehmite. The sample in Figure 7b is oxidized in steam with the conversion degree of 96.73%, has a dark gray color, and is bound with the presence of unoxidized aluminum.

Aluminum granules with a chemical purity of 99.9 and 99.7% after the oxidation experiments at 280 °C and 10 h, where the conversion degree was less than 2%, are shown in Figure 8. The oxidation process took place on the surface, without deep penetration of the chemical reaction into the granules.

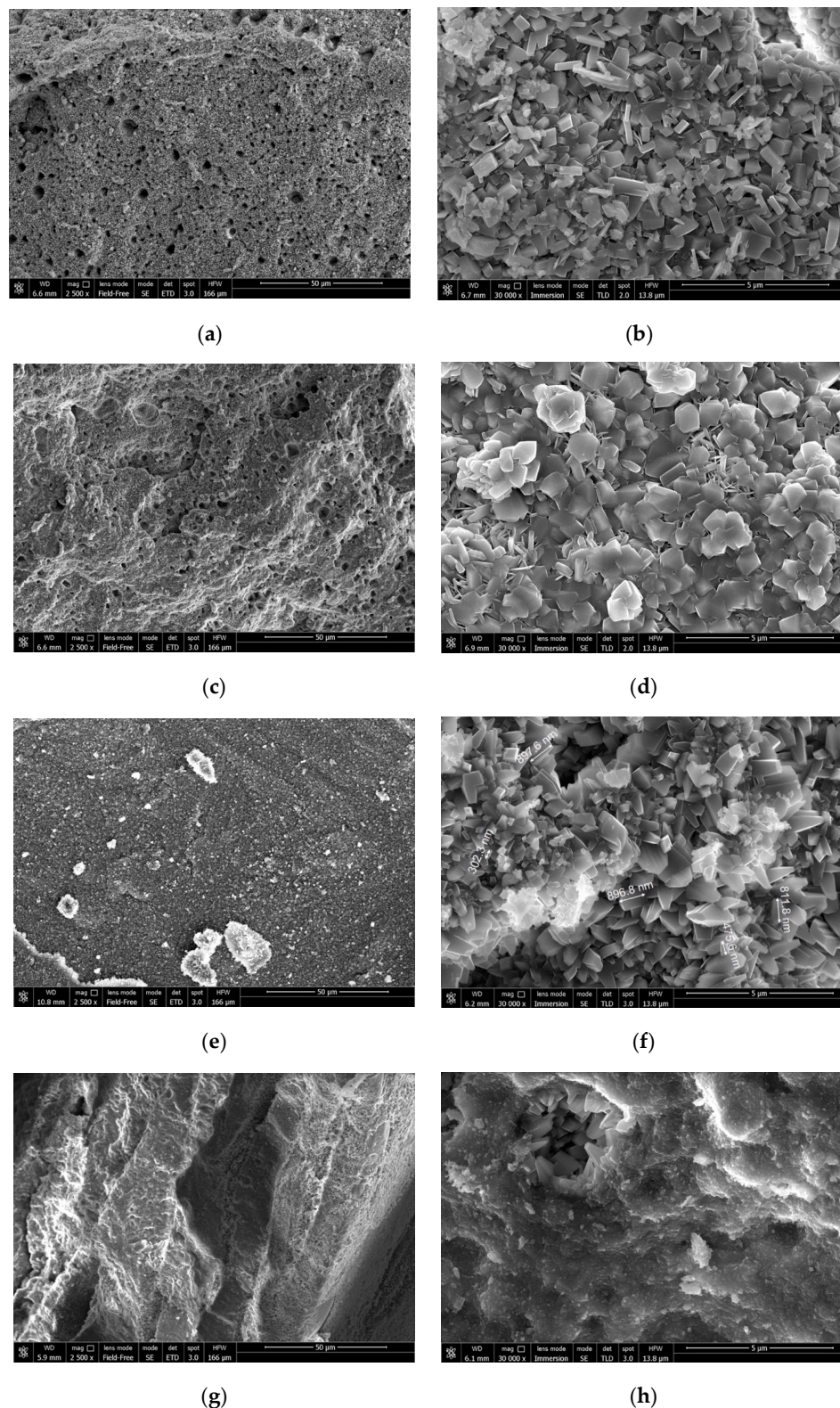


Figure 6. SEM images of boehmite obtained in oxidation experiments using 99.99% aluminum: (a) $t = 10$ h, $T = 280$ °C, steam, $\eta = 96.73\%$ (50 microns); (b) $t = 10$ h, $T = 280$ °C, steam, $\eta = 96.73\%$ (5 microns); (c) $t = 10$ h, $T = 280$ °C, liquid, $\eta = 100.0\%$ (50 microns); (d) $t = 10$ h, $T = 280$ °C, liquid, $\eta = 100.0\%$ (5 microns); (e) $t = 4$ h, $T = 280$ °C, steam, $\eta = 68.44\%$ (50 microns); (f) $t = 4$ h, $T = 280$ °C, steam, $\eta = 68.44\%$ (5 microns); (g) $t = 10$ h, $T = 240$ °C, steam, $\eta = 24.38\%$ (50 microns); (h) $t = 10$ h, $T = 240$ °C, steam, $\eta = 24.38\%$ (5 microns).



Figure 7. SEM images of boehmite obtained in oxidation experiments using 99.99% aluminum: (a) holding time = 10 h, $T = 280\text{ }^{\circ}\text{C}$, liquid, $\eta = 100.0\%$; (b) holding time = 10 h, $T = 280\text{ }^{\circ}\text{C}$, steam, $\eta = 96.73\%$.

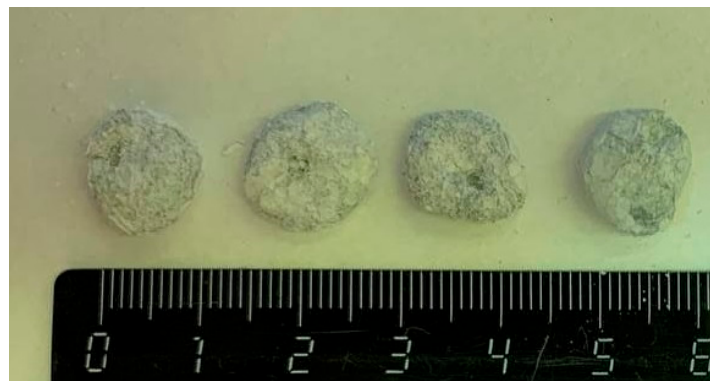


Figure 8. Photos of aluminum granules with a chemical purity of 99.9 and 99.7% after the oxidation experiments at $280\text{ }^{\circ}\text{C}$ and 10 h, with the conversion degree (η) of less than 2%.

The purity of aluminum is a critical factor in the hydrothermal oxidation process. The experiments previously outlined highlight the importance of aluminum purity for the degree of its conversion during oxidation. It was observed that aluminum with a higher chemical purity (99.99%) exhibited much more effective oxidation compared to aluminum with a lower purity (99.9% and 99.7%).

The oxidation process results in the conversion of aluminum into a compound called boehmite (AlOOH), as represented by Equation (1). When using high-purity aluminum (99.99%), nearly complete conversion to boehmite was achieved at $280\text{ }^{\circ}\text{C}$ in liquid water, whereas the conversion degree was significantly lower for aluminum of lower purity (99.9% and 99.7%), at less than 2%.

One of the factors that can explain this phenomenon is the presence of impurities such as silicon (Si), iron (Fe), copper (Cu), and magnesium (Mg) in lower purity aluminum. The concentration of these impurities is significantly higher in 99.7% and 99.9% aluminum compared to that in 99.99% pure aluminum. For instance, Si and Fe were found to be approximately 7.5 times more concentrated in 99.9% aluminum, and around 50 times more concentrated in 99.7% aluminum, as compared to the concentrations in 99.99% pure aluminum. Similarly, Cu and Mg were found in significantly higher concentrations in lower purity aluminum.

These impurities tend to accumulate near the surface of the aluminum granules and act as barriers to oxidation. They can hinder the reaction process by forming solid inclusions of boehmite on the surface, which in turn prevents the deep penetration of the chemical reaction into the granules. This could be due to the impurities forming passivation layers or themselves reacting in a manner that consumes reactants or forms phases that inhibit the oxidation of aluminum.

Moreover, it was observed that the oxidation of aluminum in liquid water is more effective than in steam as the temperature increases beyond $220\text{ }^{\circ}\text{C}$. However, the purity of

the aluminum still played a significant role in this effectiveness. High purity aluminum showed a smoother and higher conversion degree in liquid compared to that in steam.

In conclusion, the purity of aluminum is crucial for the hydrothermal oxidation process. Higher purity aluminum is more susceptible to complete or nearly complete conversion to boehmite, whereas lower purity aluminum, due to the impurities present, shows a significantly reduced conversion. These impurities appear to inhibit the oxidation reaction, especially at the surface of the aluminum granules. Therefore, for applications in which the efficient hydrothermal oxidation of aluminum is desired, it is imperative to use high-purity aluminum or to develop strategies in which other parameters for the activation of the oxidation reaction are used, i.e., mechanical activation by the intensive mixing of aluminum granules [43].

4. Conclusions

A comprehensive series of experiments were conducted on the oxidation of three different grades of aluminum granules in both distilled water and steam, with temperatures ranging from 200 °C to 280 °C, and holding times extending from 4 to 10 h.

The findings revealed a positive correlation between increasing temperature and holding time with the degree of conversion. Additionally, the chemical purity of aluminum was found to significantly impact the oxidation kinetics. Aluminum with a higher chemical purity oxidized at a notably faster rate. For instance, at a temperature of 280 °C and a holding time of 10 h, the conversion degree of granules with chemical purities of 99.9% and 99.7% was less than 2%, whereas 99.99% pure aluminum was nearly completely oxidized.

This highlights the integral role of aluminum's chemical purity in its oxidation behavior and underscores the potential for enhancing hydrogen production efficiency through optimizing aluminum purity.

Author Contributions: Experimental setup and scientific experiments, G.N.A., O.A.B. and A.V.G.; sample analysis and preparation of micrographs, G.E.V.; sample analysis and preparation of the X-ray phase, E.A.K.; writing—original draft preparation, G.N.A. and M.S.V.; writing—review and editing, V.K. All authors have read and agreed to the published version of the manuscript.

Funding: This work was supported by the Ministry of Science and Higher Education of the Russian Federation (State Assignment No. 075-01129-23-00).

Institutional Review Board Statement: Not applicable.

Informed Consent Statement: Not applicable.

Data Availability Statement: Not applicable.

Conflicts of Interest: The authors declare no conflict of interest.

References

1. Gupta, A.; Baron, G.; Perreault, P.; Lenaerts, S.; Ciocarlan, R.-G.; Cool, P.; Milo, P.; Rogge, S.; Van Speybroeck, V.; Watson, G.; et al. Hydrogen Clathrates: Next Generation Hydrogen Storage Materials. *Energy Storage Mater.* **2021**, *41*, 69–107. [[CrossRef](#)]
2. Tan, K.C.; Yu, Y.; Chen, R.; He, T.; Jing, Z.; Pei, Q.; Wang, J.; Chua, Y.S.; Wu, A.; Zhou, W.; et al. Metallo-N-Heterocycles—A new family of hydrogen storage material. *Energy Storage Mater.* **2020**, *26*, 198–202. [[CrossRef](#)]
3. Breeze, P. *Hydrogen Energy Storage. Power System Energy Storage Technologies*; Academic Press: Cambridge, MA, USA, 2018; Volume 8, pp. 69–77.
4. Davies, J.; Du Preez, S.P.; Bessarabov, D.G. The Hydrolysis of Ball-Milled Aluminum–Bismuth–Nickel Composites for On-Demand Hydrogen Generation. *Energies* **2022**, *15*, 2356. [[CrossRef](#)]
5. Saceleanu, F.; Vuong, T.V.; Master, E.R.; Wen, J.Z. Tunable kinetics of nanoaluminum and microaluminum powders reacting with water to produce hydrogen. *Int. J. Environ. Res.* **2019**, *43*, 7384–7396. [[CrossRef](#)]
6. Hiraki, T.; Yamauchi, S.; Iida, M.; Uesugi, H.; Akiyama, T. Process for Recycling Waste Aluminum with Generation of High-Pressure Hydrogen. *Environ. Sci. Technol.* **2007**, *41*, 4454–4457. [[CrossRef](#)] [[PubMed](#)]
7. Olivares-Ramírez, J.M.; Castellanos, R.H.; de Jesús, Á.M.; Borja-Arco, E.; Pless, R.C. Design and Development of a Refrigeration System Energized with Hydrogen Produced from Scrap Aluminum. *Int. J. Hydrogen Energy* **2008**, *33*, 2620–2626. [[CrossRef](#)]
8. Liu, H.; Yang, F.; Yang, B.; Zhang, Q.; Chai, Y.; Wang, N. Rapid Hydrogen Generation through Aluminum-Water Reaction in Alkali Solution. *Catal. Today* **2018**, *318*, 52–58. [[CrossRef](#)]

9. Ho, C.Y. Hydrolytic Reaction of Waste Aluminum Foils for High Efficiency of Hydrogen Generation. *Int. J. Hydrogen Energy* **2017**, *42*, 19622–19628. [[CrossRef](#)]
10. Macanás, J.; Soler, L.; Candela, A.M.; Muñoz, M.; Casado, J. Hydrogen Generation by Aluminum Corrosion in Aqueous Alkaline Solutions of Inorganic Promoters. *Energy* **2011**, *36*, 2493–2501. [[CrossRef](#)]
11. Chai, Y.J.; Dong, Y.M.; Meng, H.X.; Jia, Y.Y.; Shen, J.; Huang, Y.M.; Wang, N. Hydrogen Generation by Aluminum Corrosion in Cobalt (II) Chloride and Nickel (II) Chloride Aqueous Solution. *Energy* **2014**, *68*, 204–209. [[CrossRef](#)]
12. Shchurin, V.N.; Baev, A.K.; Tishevich, V.I. Zeolite Modification with Aluminum and Efficiency of Gas Purification. *Russ. J. Appl. Chem.* **2002**, *75*, 1252–1255. [[CrossRef](#)]
13. Kravchenko, O.V.; Semenenko, K.N.; Bulychev, B.M.; Kalmykov, K.B. Activation of Aluminum Metal and its Reaction with Water. *J. Alloys Compd.* **2005**, *397*, 58–62. [[CrossRef](#)]
14. Fan, M.-Q.; Sun, L.-X.; Xu, F. Experiment Assessment of Hydrogen Production from Activated Aluminum Alloys in Portable Generator for Fuel Cell Applications. *Energy* **2010**, *35*, 2922–2926. [[CrossRef](#)]
15. Liu, Y.; Wang, X.; Liu, H.; Dong, Z.; Li, S.; Ge, H.; Yan, M. Improved Hydrogen Generation from the Hydrolysis of Aluminum Ball Milled with Hydride. *Energy* **2014**, *72*, 421–426. [[CrossRef](#)]
16. Yang, W.; Zhang, T.; Zhou, J.; Shi, W.; Liu, J.; Cen, K. Experimental Study on the Effect of Low Melting Point Metal Additives on Hydrogen Production in the Aluminum–Water Reaction. *Energy* **2015**, *88*, 537–543. [[CrossRef](#)]
17. Liu, Y.; Wang, X.; Liu, H.; Dong, Z.; Li, S.; Ge, H.; Yan, M. Investigation on the Improved Hydrolysis of Aluminum–Calcium Hydride-Salt Mixture Elaborated by Ball Milling. *Energy* **2015**, *84*, 714–721. [[CrossRef](#)]
18. Liu, Y.; Wang, X.; Liu, H.; Dong, Z.; Li, S.; Ge, H.; Yan, M. Effect of Salts Addition on the Hydrogen Generation of Al–LiH Composite Elaborated by Ball Milling. *Energy* **2015**, *89*, 907–913. [[CrossRef](#)]
19. Wang, H.; Wang, Z.; Shi, Z.; Gong, X.; Cao, J.; Wang, M. Facile Hydrogen Production from Al–Water Reaction Promoted by Choline Hydroxide. *Energy* **2017**, *131*, 98–105. [[CrossRef](#)]
20. Xiao, F.; Guo, Y.; Li, J.; Yang, R. Hydrogen Generation from Hydrolysis of Activated Aluminum Composites in Tap Water. *Energy* **2018**, *157*, 608–614. [[CrossRef](#)]
21. Xiao, F.; Yang, R.; Li, J. Hydrogen Generation from Hydrolysis of Activated Aluminum/Organic Fluoride/Bismuth Composites with High Hydrogen Generation Rate and Good Aging Resistance in Air. *Energy* **2019**, *170*, 159–169. [[CrossRef](#)]
22. Guan, X.; Zhou, Z.; Luo, P.; Wu, F.; Dong, S. Hydrogen Generation from the Reaction of Al-Based Composites Activated by Low-Melting-Point Metals/Oxides/Salts with Water. *Energy* **2019**, *188*, 116107. [[CrossRef](#)]
23. Hou, K.; Hou, X.; Ye, X.; Li, D.; Suo, G.; Xie, L.; Shu, Q.; Cao, Q.; Bai, J. Carbon Nanotubes and (Mg₁₀Ni)₈₅Ce₁₅ Synergistically Activate Mg–Al Alloy Waste for Efficiently Hydrolysis Hydrogen Generation. *Fuel* **2022**, *324*, 124829. [[CrossRef](#)]
24. Li, D.; Cai, Y.; Chen, C.; Lin, X.; Jiang, L. Magnesium–Aluminum Mixed Metal Oxide Supported Copper Nanoparticles as Catalysts for Water–Gas Shift Reaction. *Fuel* **2016**, *184*, 382–389. [[CrossRef](#)]
25. He, T.; Chen, W.; Wang, W.; Du, S.; Deng, S. Microstructure and Hydrogen Production of the Rapidly Solidified Al–Mg–Ga–In–Sn Alloy. *J. Alloys Compd.* **2020**, *827*, 154290. [[CrossRef](#)]
26. Amrani, M.A.; Haddad, Y.; Obeidat, F.; Ghaleb, A.M.; Mejjaoui, S.; Rahman, I.; Galil, M.S.A.; Shameeri, M.; Alsofi, A.A.; Saif, A. Productive and Sustainable H₂ Production from Waste Aluminum Using Copper Oxides-Based Graphene Nanocatalysts: A Techno-Economic Analysis. *Sustainability* **2022**, *14*, 15256. [[CrossRef](#)]
27. Chen, X.; Wang, C.; Liu, Y.; Chen, Y.; Zhang, Q.; Yang, S.; Lu, H.; Zhou, H.; Lin, K.; Liu, H.; et al. Popcorn-Like Aluminum-Based Powders for Instant Low-Temperature Water Vapor Hydrogen Generation. *Mater. Today Energy* **2021**, *19*, 100602. [[CrossRef](#)]
28. Buryakovskaya, O.A.; Suleimanov, M.Z.; Vlaskin, M.S.; Kumar, V.; Ambaryan, G.N. Aluminum Scrap to Hydrogen: Complex Effects of Oxidation Medium, Ball Milling Parameters, and Copper Additive Dispersity. *Metals* **2023**, *13*, 185. [[CrossRef](#)]
29. Vlaskin, M.S.; Grigorenko, A.V.; Zhuk, A.Z.; Lisitsyn, A.V.; Sheindlin, A.E.; Shkolnikov, E.I. Synthesis of High-Purity α -Al₂O₃ from Boehmite Obtained by Hydrothermal Oxidation of Aluminum. *High Temp.* **2016**, *54*, 322–329. [[CrossRef](#)]
30. Zhuk, A.Z.; Vlaskin, M.S.; Grigorenko, A.V.; Kislenco, S.A.; Shkolnikov, E.I. Synthesis of High-Purity α -Al₂O₃ from Boehmite by High Temperature Vacuum Treatment. *J. Ceram. Process. Res.* **2016**, *17*, 910–918.
31. Kislenco, S.A.; Vlaskin, M.S.; Zhuk, A.Z. Diffusion of Cation Impurities by Vacancy Mechanism in α -Al₂O₃: Effect of Cation Size and Valence. *Solid State Ionics* **2016**, *293*, 1–6. [[CrossRef](#)]
32. Bersh, A.V.; Lisitsyn, A.V.; Sorokovikov, A.I.; Vlaskin, M.S.; Mazalov, Y.A.; Shkolnikov, E.I. Study of the Processes of Steam–Hydrogen Mixture Generation in a Reactor for Hydrothermal Aluminum Oxidation for Power Units. *High Temp.* **2010**, *48*, 866–873. [[CrossRef](#)]
33. Vlaskin, M.S.; Shkolnikov, E.I.; Bersh, A.V. Oxidation Kinetics of Micron-Sized Aluminum Powder in High-Temperature Boiling Water. *Int. J. Hydrogen Energy* **2011**, *36*, 6484–6495. [[CrossRef](#)]
34. Vlaskin, M.S.; Shkolnikov, E.I.; Bersh, A.V.; Zhuk, A.Z.; Lisitsyn, A.V.; Sorokovikov, A.I.; Pankina, Y.V. An Experimental Aluminum-Fueled Power Plant. *J. Power Sources* **2011**, *196*, 8828–8835. [[CrossRef](#)]
35. Vlaskin, M.S.; Valyano, G.E.; Zhuk, A.Z.; Shkolnikov, E.I. Oxidation of Coarse Aluminum in Pressured Water Steam for Energy Applications. *Int. J. Environ. Res.* **2020**, *44*, 8689–8715. [[CrossRef](#)]
36. Escobar-Alarcón, L.; Iturbe-García, J.L.; González-Zavala, F.; Solís-Casados, D.A.; Pérez-Hernández, R.; Haro-Poniatowski, E. Hydrogen Production by Ultrasound Assisted Liquid Laser Ablation of Al, Mg and Al–Mg Alloys in Water. *Appl. Surf. Sci.* **2019**, *478*, 189–196. [[CrossRef](#)]

37. Xu, F.; Sun, L.; Lan, X.; Hu, H.; Sun, Y.; Zhou, H.; Li, F.; Yang, L.; Si, X.; Zhang, J.; et al. Mechanism of Fast Hydrogen Generation from Pure Water Using Al–SnCl₂ and Bi-doped Al–SnCl₂ Composites. *Int. J. Hydrogen Energy* **2014**, *39*, 5514–5521. [[CrossRef](#)]
38. Jia, Y.; Shen, J.; Meng, H.; Dong, Y.; Chai, Y.; Wang, N. Hydrogen Generation Using a Ball-milled Al/Ni/NaCl Mixture. *J. Alloys Compd.* **2014**, *588*, 259–264. [[CrossRef](#)]
39. He, T.; Chen, W.; Wang, W.; Ren, F.; Stock, H.-R. Effect of Different Cu Contents on the Microstructure and Hydrogen Production of Al–Cu–Ga–In–Sn Alloys for Dissolvable Materials. *J. Alloys Compd.* **2020**, *821*, 153489. [[CrossRef](#)]
40. Soler, L.; Candela, A.M.; Macanás, J.; Muñoz, M.; Casado, J. Hydrogen Generation by Aluminum Corrosion in Seawater Promoted by Suspensions of Aluminum Hydroxide. *Energy* **2009**, *34*, 8511–8518. [[CrossRef](#)]
41. Ziebarth, J.T.; Woodall, J.M.; Kramer, R.A.; Choi, G. Liquid Phase-enabled Reaction of Al–Ga and Al–Ga–In–Sn Alloys with Water. *Int. J. Hydrogen Energy* **2011**, *36*, 5271–5279. [[CrossRef](#)]
42. Lim, S.T.; Sethupathi, S.; Alsultan, A.G.; Munusamy, Y. Hydrogen Production via Activated Waste Aluminum Cans and Its Potential for Methanation. *Energy Fuels* **2021**, *35*, 16212–16221. [[CrossRef](#)]
43. Ambaryan, G.N.; Vlaskin, M.S.; Dudoladov, A.O.; Meshkov, E.A.; Zhuk, A.Z.; Shkolnikov, E.I. Hydrogen Generation by Oxidation of Coarse Aluminum in Low Content Alkali Aqueous Solution under Intensive Mixing. *Int. J. Hydrogen Energy* **2016**, *41*, 17216–17224. [[CrossRef](#)]

Disclaimer/Publisher’s Note: The statements, opinions and data contained in all publications are solely those of the individual author(s) and contributor(s) and not of MDPI and/or the editor(s). MDPI and/or the editor(s) disclaim responsibility for any injury to people or property resulting from any ideas, methods, instructions or products referred to in the content.